International Journal of Nanoelectronics and Materials
Volume 11, No. 2, Apr 2018 [195-210]

Aluminum Incorporation Impacts on Some Physical Properties of Pure CdO Film Synthesized by Spray Pyrolysis

Ninet M. Ahmed[a], Hassan H. Afify[b*] and Fatma M. Ibrahim[c]

[a]*Photovoltaic Department, Electronics Research Institute, Dokki, Egypt.*
[b]*Solid State Lab., National Research Centre, Dokki, Egypt.*
[c]*Physics Department, Faculty of Science, Mansoura University, Egypt.*

Received 27 September 2017; Revised 11 December 2017; Accepted 2 January 2018

ABSTRACT

Transparent conducting for pure and incorporated aluminum cadmium oxide (CdO:Al) thin films was prepared using spray pyrolysis method at a substrate temperature of 425 °C and a spray time of 25 minutes. The effects of Al incorporation on structural, optical, and electrical properties as well as surface morphology of the prepared films were inverstigated as a function of aluminum concentration. Calculations of crystallite size, dislocation density, as well as microstrain based on XRD patterns of the samples were performed. The incorporated Al induces a significant decrease in peaks' intensity and changes the preferred orientation. The band gap energy varies from 2.45 eV to 2.57 eV, depending on the Al concentration. Low refractive index (n) is achieved for CdO:Al samples. The sheet resistance measurements demonstrate an observable increase and decrease with Al incorporation.

Keywords: CdO & CdO, Al Thin Films, Structure, Optical, Sheet Resistance, Figure of Merit, Spray Pyrolysis.

1. INTRODUCTION

Transparent conducting oxide (TCO) thin films have great potential in optoelectronic applications. Among the TCOs, cadmium oxide (CdO) is a promising material in this field especially for solar cells [1-2], photodetectors [3], light emitting diodes [4], transparent electrodes [5], and gas sensors [6] due to its high optical transmittance and electrical conductivity privileges. In addition, CdO films have a wide, direct band gap ranged from 2.2 eV to 2.8 eV [7]. Pure CdO films can be doped with some metallic ions such as Al [8-11], In [12-13], F [14-15], Cr [16], Te [17], Sn [18], Fe [19], Mn [20], Ga [21], Mg [22], Zn [23], B [24], and Cu [3] during the deposition process as an improvement factor. In this context, there is no consensus in published data as they are diverged. Moreover, most of the obtained results from same and different techniques are debatable. There is no consensus on which doping element is the best. Therefore, more studies are needed.

Many techniques based on physical and chemical concepts have been adapted to deposit pure and doped CdO films such as sol–gel [25-27], SILAR [28], thermal evaporation [29], electron beam evaporation [30], pulsed laser deposition [31], sputtering [32], chemical vapour deposition [33], elctrodeposition [34], and spray pyrolysis [35-36]. Each technique is characterized by its disadvantages and merit. However, the spray pyrolysis technique is advantageous over other techniques since it is simple, is inexpensive, uses low processing temperature, is a vacuumless system, is easy for industrial fabrication, is easy to add a doping

*Corresponding Author: hassanafify@ymail.com

material, has good reproducibility, has high growth rate and homogeneity of film surface [37]. Therefore, this method was adopted here and installed to prepare both pure and Al incorporated CdO thin films with various Al content (at 0, 1, 2, 3, 4, and 5%), in the present study. The influence of Al concentration on the structure, morphology, and optical and electrical properties of pure & CdO:Al films were investigated via XRD, AFM, UV-VIS-NIR spectroscopy and two probe method respectively.

2. EXPERIMENTAL DETAILS

2.1 Sample Preparation

Pure and Al incorporated CdO thin films were deposited on Corning 7059 glass substrates by spray pyrolysis technique at a substrate temperature of 425 °C and a spray time of 25 min. The spray set-up is described elsewhere [38]. The substrates were cleaned with detergent, degreased with acetone, and rinsed with bi-distilled water in an ultrasonic cleaner. CdO thin films were prepared from 0.1M solution of cadmium acetate dihydrate [Cd $(COOCH_3)_2 \cdot 2H_2O$] dissolved in a mixture of methanol and bi-distilled water (1:1). The Al incorporated CdO thin films were obtained through the preparation of 0.1M aluminium nitrate [$Al(NO_3)_3 \cdot 9H_2O$] solution dissolved in a mixture of bi-distilled water and methanol (1:1). Then, this solution was added to the mother Cd solution at different volume ratios (1%, 2%, 3%, 4%, 5%). The predetermined optimum spray parameters were fixed at their optimum values: the distance between the nozzle and the substrate surface was 35cm, the air flow rate was 20L/min, and the flow rate of the solution was 1.32 ml/min. The temperature of the substrate was controlled within $\pm$ 2°C using a chrome-nickel thermocouple that is used as a sensor for the temperature controller. The thermocouple was hold tightly beneath the substrate on the hot plate surface. The spray process started after 20 minutes after laying the glass substrate on the hot plate surface to ensure that it attained the required temperature.

3. SAMPLE CHARACTERIZATION

Samples structure was elucidated by analyzing their X-ray diffraction patterns (XRD) using a Philips (PW-1710) diffractometer. Data were recorded in the 2θ range from 10º to 80º with a step size of 0.02° using Cu-Kα radiation (λ=1.54056Å). Surface morphology was visualized using an AFM ZYGO Maxim-GP 200 profilometer. Specular transmittance and reflectance were measured by a double beam spectrophotometer to calculate the refractive index (n) and energy gap (Eg). Sheet resistance was measured using the two-probe method with a DC power supply GW INSTEK -GPQ-3020D, and two high resolution multimeters EXECH instruments EX530 to determine the sheet resistance and figure of merit.

3.1 Structural Properties

3.1.1 X-ray Diffraction Patterns

The X-ray diffraction patterns of unincorporated and Al incorporate CdO thin films with different concentrations (1-5 %) by volume that were deposited at a fixed substrate temperature of 425ºC and a spray time of 25 min. are shown in Figure 1. The salient features of Figure 1 are: (i) No change is observed in peaks' position due to the Al incorporation. (ii) The preferred orientation plane changes from (200) for pure CdO film to (111) for the incorporated samples. (iii) The peaks' intensity of Al incorporated CdO films show a significant non-systematic change when the Al concentration increases from 1 to 5 %. The obtained X-ray diffraction spectra were indexed with JCPDS files. It is found that the obtained 2θ and the

corresponding d values are, to a great extent, compatible with those existed in the JCPDS card No. 005-0640. The planes corresponding to the 2θ (32.99, 38.25, 55.25, 65.90, 69.28) are (111), (200), (220), (311), and (222). The XRD patterns for the investigated samples have no additional peaks related to pure Al or its compounds upon the Al incorporation. The JCPDS card No. 005-0640 reference indicates that the prepared samples are polycrystalline with a face centered cubic (FCC) crystal structure.

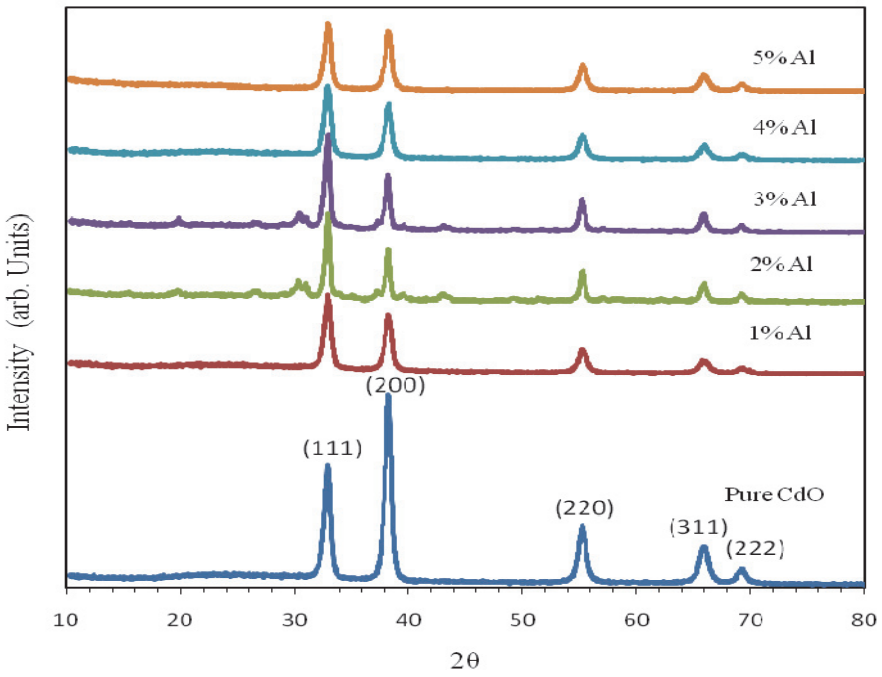

Figure 1. XRD patterns for pure CdO, and 1-5% Al incorporated samples deposited at 425ºC and 25 min.

The incorporation of CdO films with Al causes a drastic reduction in the intensity of (200) and (111) peaks. The (111) peak emerges as the strongest one. Therefore, the preferential orientation is shifted from the (200) to the (111) growth direction. Increasing the concentration of incorporated Al shows a slight change in the intensity of (200) and (111) peaks. However, the decrease in peaks' intensity is probably due to the decrease in crystallinity and the change in growth direction. This behavior is consistent with that reported by R. Kumaravel *et al*. for CdO:In thin layer deposited using spray pyrolysis method [13] .

3.1.2. Calculation of Structure Parameters Based on XRD Patterns

It is possible to calculate some structure parameters based on XRD patterns such as crystallite size (D), microstrain (ε), dislocation density (δ), lattice constant (a), and the inter planer distance (d) to obtain more information about the structure characteristics of pure and Al-incorporated CdO films.

The crystallite size and microstrain of the CdO layer as a function of Al concentration can be estimated using the Williamson-Hall equation [39]

$$\frac{\beta \cos\theta}{\lambda} = \frac{1}{D} + \frac{\varepsilon \sin\theta}{\lambda} \quad (1)$$

Where λ (1.5406Å) is the wave length of X-rays, β is the full width at half-maximum of the diffraction (radian), and θ is the diffraction angle (degree). The plot of $\beta \cos\theta/\lambda$ vs $\sin\theta/\lambda$ of

CdO thin film as a function of Al concentration is shown in Figure 2. The slope of the plot gives the microstrain and the inverse of the intercept on the y-axis gives the crystallite size value.

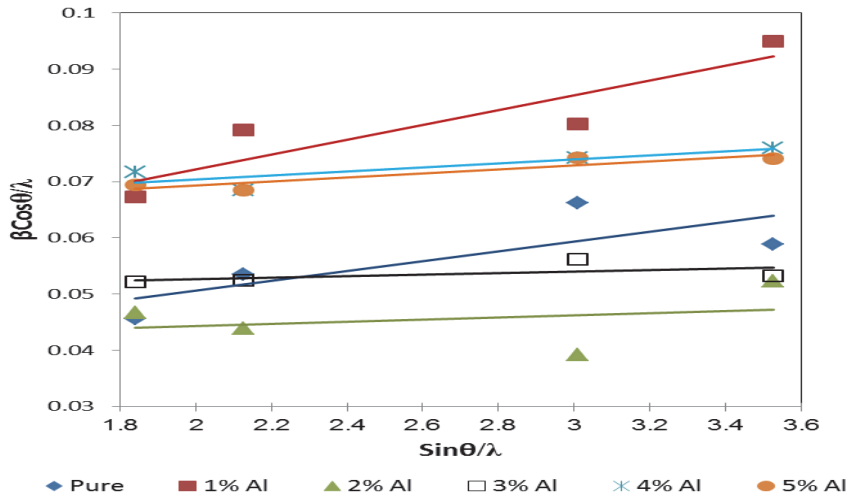

Figure 2. Williamson–Hall plot to determine crystallite size and microstrain of CdO film prepared at different Al concentrations.

The estimated values of crystallite size as a function of Al concentration are shown in Figure 3 and listed in Table 1. It is observed that, the values of samples' crystallite size are shown to be diminishing with increasing Al concentration. This could be attributed to the roughly 23% difference in radius between cadmium (0.074nm) and aluminum (0.057nm). The interstitial Al and segregated Al at crystallite boundaries induce internal strains conjugated with more probable impedance of crystallite growth, which allows the diminishing of the crystallite size.

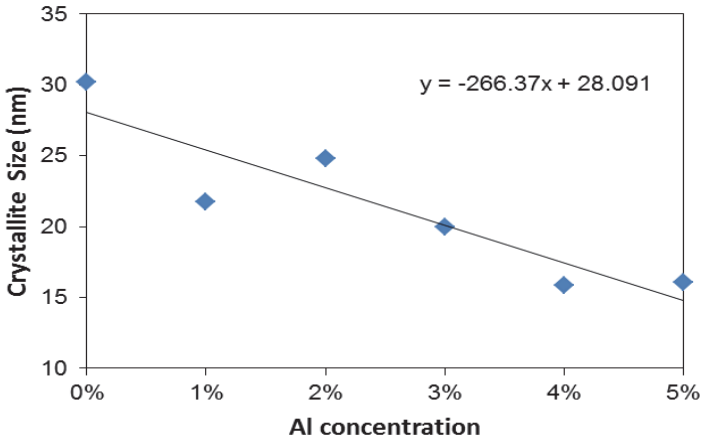

Figure 3. Variation of crystallite size with Al concentration.

The obtained data for the microstrain are not ordered. When these data were subjected to fitting, a straight line with negative slope is produced. This means that the microstrain reduces with the increase in Al concentration, which is not expected. The calculated values of the microstrain as a function of Al concentration are shown in Figure 4 and listed in Table 1.

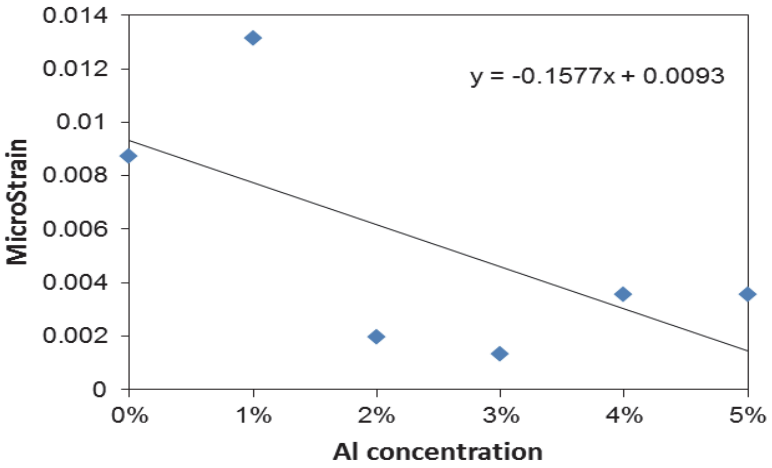

Figure 4. Variation of microstrain with Al concentration.

The dislocation density (δ) is specified by the dislocation lines' length in unit volume of the particle. It could be calculated by the concept of Williamson and Smallman as [12, 18].

$$\delta = \frac{1}{D^2} \tag{2}$$

The dislocation density variation with the Al doping concentration is shown in Figure 5. The dislocation density increases with increasing Al incorporation as a result of the decrease in crystallite size D.

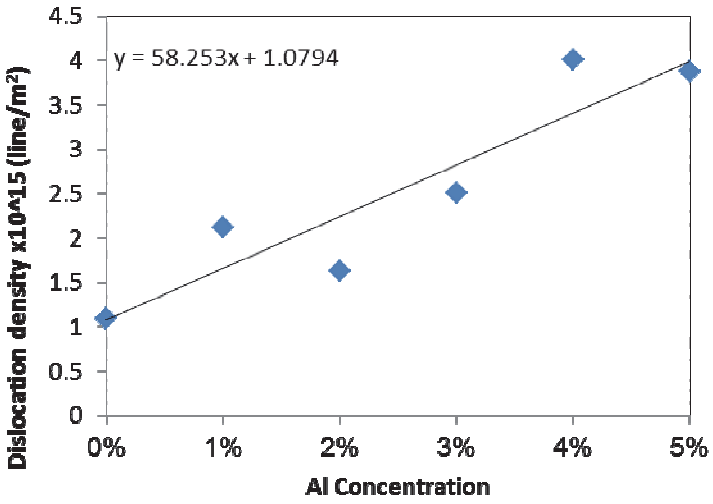

Figure 5. Variation of dislocation density with Al concentration.

A comparison of the estimated values of crystallite size, microstrain, and dislocation density of pure and CdO:Al thin films between the present work and other works is presented in Table 1. In the present study, it is observed that pure CdO films posses the maximum value of crystallite size and minimum value of dislocation density. This behavior is consistent with previous reports by Helen *et al*. [40] and by C. Aydinm and co-workers [26]. The calculated values of microstrain are reduced with Al incorporation (exception of 1% Al concentration), which conflicts with the behavior reported by Helen *et al*. and Aydin and co-workers. The values of the crystallite size, microstrain, and dislocation density that are listed in Table 1 indicate that,

the variation of these parameters is not systematic with the dopant concentration. Therefore, it is difficult to correlate the variation of these parameters with incorporated Al's percentage.

Table 1 The crystallite size (D), microstrain (ε) and dislocation density (δ) of pure CdO and CdO:Al thin films

Percentage Doping (%)	**Present Work**			**CdO:Al spray pyrolysis [40]**			**CdO:Al sol-gel [26]**		
	D_{W-H} (nm)	Microstrain ($\times 10^{-3}$)	Dislocation density ($\times 10^{15}$) lines m^{-2}	D_{W-H} (nm)	Microstrain ($\times 10^{-3}$)	Dislocation density ($\times 10^{15}$) lines m^{-2}	D (nm)	Microstrain ($\times 10^{-3}$)	Dislocation density ($\times 10^{15}$) lines m^{-2}
0	30.21	8.74	1.097	17	1.9771	3.246	17.2	117.457	3.380
1	21.74	13.13	2.115	-	-	-	-	-	-
2	24.77	1.95	1.629	-	-	-	-	-	-
3	19.98	1.32	2.505	15	2.1830	3.960	-	-	-
4	15.81	3.56	4.000	-	-	-	-	-	-
5	16.08	3.57	3.867	15	2.3068	4.420	15.9	124.165	3.956
10	-	-	-	16	2.0594	3.522	16.1	122.875	3.853
15	-	-	-	12	2.8831	6.898	16.3	121.155	3.764
20	-	-	-	-	-	-	16.8	118.321	3.543

The lattice constant 'a' of the (111) and (200) peaks were calculated using the following equation [25]:

$$a = d_{hkl}(h^2 + k^2 + l^2)^{1/2} \quad (3)$$

Where d_{hkl} is the inter-planer spacing, which is calculated from Bragg's law. The calculated values for the investigated samples and those present in the JCPDS card No. 005-064 are tabulated in Tables (2 and 3). The results show that the calculated "d" and "a" values for all deposited films are very close to the standard values reported in the JCPDS card No. 005-0640.

A comparison of the calculated values for the structural parameters of pure and CdO:Al thin films between the present work and other works is presented in Tables (2 and 3). It is observed that the obtained values are comparable with the previously published work of pure and CdO:Al layers deposited using the spray pyrolysis method [8, 40].

Table2 The diffraction angle and the structural parameters of (111) peak for pure and incorporated with different Al concentrations

2θ & LATTICE PARAMETERS		AL CONCENTRATION (%)						
		Pure	**1%**	**2%**	**3%**	**4%**	**5%**	**Ref.**
2θ	Standard (32.002°)	32.99°	32.89°	32.90°	32.87°	32.88°	32.90°	Present work
d(Å)	Standard (2.712 Å)	2.714	2.722	2.721	2.723	2.723	2.721	
a (Å)	Standard (4.6953Å)	4.700	4.714	4.713	4.717	4.716	4.712	
2θ	Standard (33. 00°)	32.94°	33.04°	32.90°	33.22°	**----**	**----**	CdO:Al [8]
d(Å)	Standard (2.712 Å)	2.717	2.709	2.720	2.695	-----	------	
a (Å)	Standard (4.695Å)	4.706	4.692	4.712	4.667	-------	-------	
2θ	Standard (33.001°)	32.922°	33.1649°	---	32.969°	------	33.5310°	CdO:Al [40]
d(Å)	Standard (2.7120Å)	2.792	2.6994	-------	2.750	------	2.6705	
a (Å)	Standard (4.695Å)	4.6263	4.6745	-------	4.76313	-------	4.6252	

Table 3 The diffraction angle and the structural parameters of (200) peak for pure and incorporated with different Al concentrations

2θ & LATTICE PARAMETERS		AL CONCENTRATION (%)						
		Pure	**1%**	**2%**	**3%**	**4%**	**5%**	**Ref.**
2θ	Standard (38.286°)	38.25°	38.22°	38.20°	38.18°	38.21°	38.24°	Present work
d(Å)	Standard (2.34 9Å)	2.352	2.353	2.355	2.356	2.356	2.352	
a (Å)	Standard (4.6953Å)	4.703	4.707	4.710	4.712	4.708	4.705	
2θ	Standard (38. 29°)	38.24°	38.36°	38.14°	38.40°	----	------	CdO:Al [8]
d(Å)	Standard (2.349Å)	2.352	2.345	2.358	2.342	-----	------	
a (Å)	Standard (4.695Å)	4.703	4.689	4.715	4.685	-------	-------	
2θ	Standard (38.29°)	37.942°	37.701°	---	38.5658°	------	38.190°	CdO:Al [40]
d(Å)	Standard (2.349Å)	2.349	2.3840	-------	2.3327	------	2.355	
a (Å)	Standard (4.695Å)	4.6263	4.6745	-------	4.76313	-------	4.6252	

The incorporated Al on CdO lattice is prone to inset in the interstitial sites since the ionic radius of an Al ion is less than that of a Cd ion by 23%. As the Al concentration increases, the interstitial and the equivalent sites are sequentially filled and the excess diffuse towards the crystallite boundaries. As a result, lattice deformation takes place, inducing a deterioration in crystallinity and crystallite growth impedance, which give rise to an increase in dislocation density. The obtained XRD patterns and AFM images support this view.

3.1.3 Surface Morphology

The two (2D) and three-dimensional (3D) AFM images of the surface morphology over a scanning area of 5μm×5μm of pure CdO and 2% and 4% Al incorporated samples as examples are shown in Figure 6. The AFM images of pure CdO film show nearly rounded crystallites surrounded with black spots that represent voids or cavities. The crystallites tend to gather to form clusters with different irregular shapes, sizes, and separation as a result of the Al incorporation. These morphological changes could be referred to the change in preferred growth orientation from (200) to (111). The CdO:Al samples indicate the lowest crystallite size. The white regions in the AFM images represent the formation of agglomerated crystallite. The surface roughness of the samples increases with the increase in Al concentration up to 2% and decreases with further increase in the concentration of Al to 4%. The change of growth direction from (200) for pure CdO to (111) for CdO:Al may be the main cause for the observed reasonable roughness in the incorporated CdO:Al samples up to 2%. The roughness (rms) values of pure and CdO:Al films are given in Table 4.

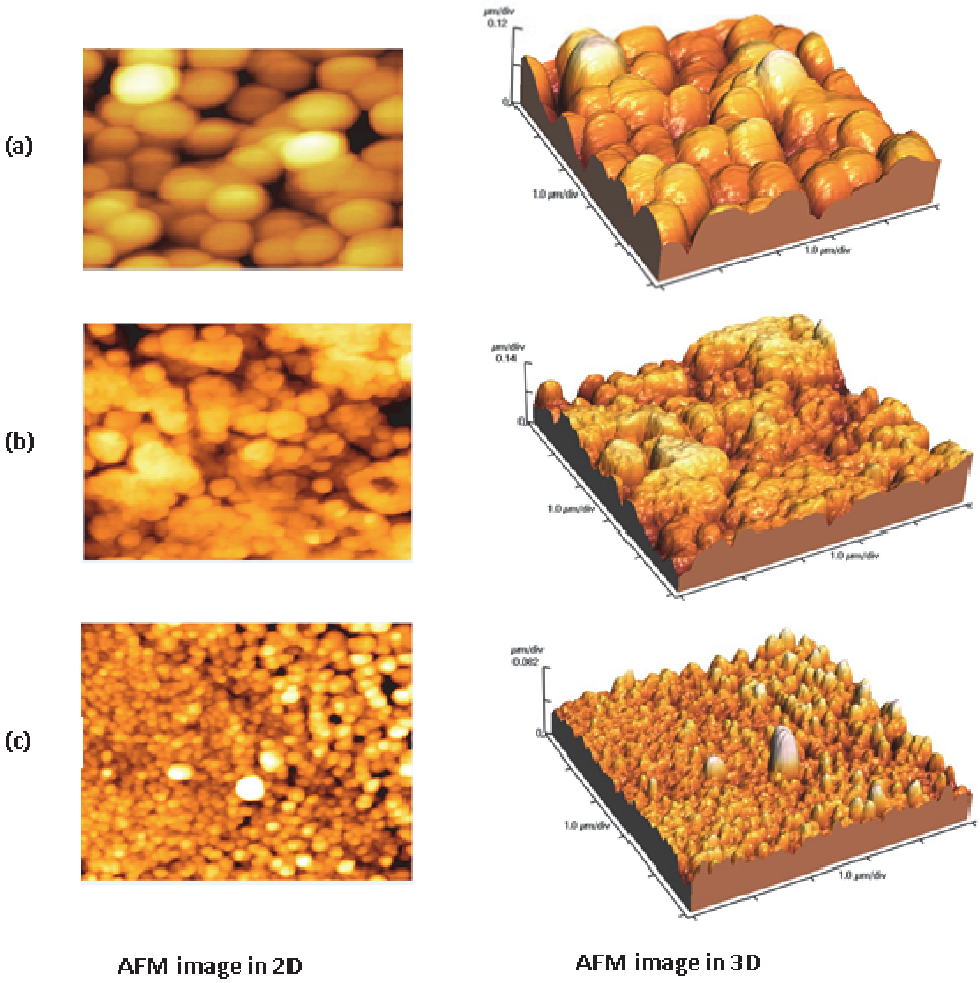

Figure 6. 2D & 3D AFM images of pure and CdO:Al thin film (a) pure CdO, (b) 2%Al and (c) 4% Al.

Table 4 Roughness values for pure and CdO:Al layes with different Al concentrations

Al concentrations	Roughness (rms) (nm)
0%	26.93
2%	34.25
4%	9.530

The obtained lesser roughness as a result of excess Al incorporation may be due to the ordered stack and packing of the produced small crystallites.

3.2 Optical Properties

3.2.1 Transmittance

The optical transmittance spectra of pure and CdO:Al thin films deposited on glass substrates with different Al concentrations are shown in Figure 7. This figure shows three distinct stages with the first one related to the energy gap, which exists in the short wavelength range (250-600nm). Sharp absorption edge is observed with slight changes corresponding to the increase in Al concentration. The second stage is related to the effect of film thickness and founded in the range (600-1500nm). The third one is characterized by an observable decrease in transmittance at the long wavelength range (1500-2500nm). This decrease is related to the free electrons absorption resulted from Al incorporation, which is consistent with published data [11, 20, 23].

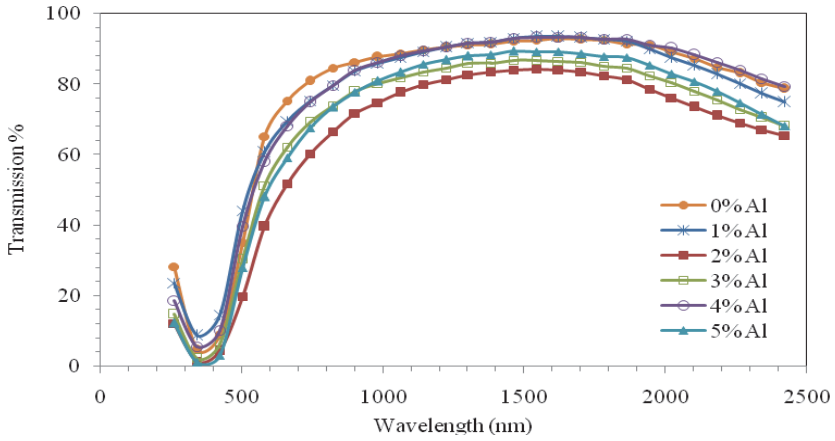

Figure 7. Transmittance of pure and CdO:Al thin films with different Al concentrations.

The variation of average transmittance in the 600nm to 1500nm region with Al concentration is shown in Figure 8. It is clear that the change is not systematic. The decreasing trend of the transmittance with increasing Al concentration up to 2% could be attributed to the probable increase in both film thickness and surface roughness caused by the change in growth direction. The increasing trend of the transmittance beyond 2% Al concentration is probably due to the increase in energy gap based on the BRUSTEIN-MOSS effect [21].

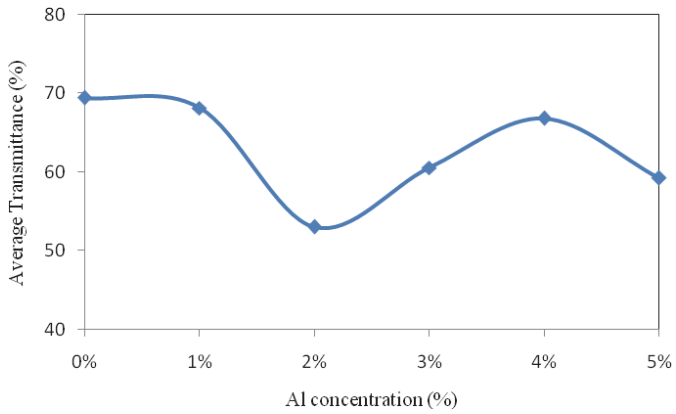

Figure 8. Variation of average transmittance of pure and CdO:Al thin films with different Al concentrations.

3.2.2 Reflectance

The variation of reflectance with wavelength for pure and CdO:Al layers of various Al concentrations is shown in Figure 9. All samples show normal reflectance spectra. The most obvious feature is the reasonable increases in reflectance in the wavelength range of 2000-2500nm, which increases with the increase in Al concentration.

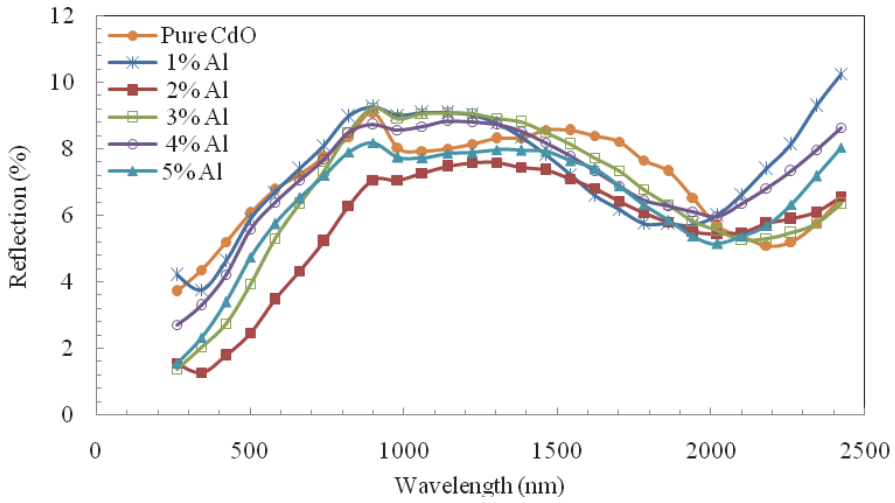

Figure 9. Variation of reflectance with wavelength for pure and CdO:Al with different Al concentrations.

3.2.3 Band Gap Energy

The direct optical energy gap is visualized as the direct transition between valence and conduction bands. The absorption coefficient (α) was calculated using this formula: $\alpha = \frac{1}{d}\ln(\frac{1}{T})$ where T is the transmittance and d is the film thickness. The absorption coefficient and the incident photon energy (hυ) are related by the following equation [29-31]:

$$(\alpha h\upsilon)^2 = A(h\upsilon - E_g) \tag{4}$$

Where A is a constant and E_g is the band gap energy of the material. The direct optical band gap energy was calculated by extending the linear part of the curve $(\alpha h\upsilon)^2$ against (hυ) to the point

where αhν = 0. The plot of $(\alpha h\nu)^2$ vs. (hν) for pure and CdO:Al films is shown in Figure 10. It was performed to calculate the energy gap of the investigated samples.

The variation of the band gap energy with Al concentration is shown in Figure 11. The increase in the energy gap from the Al incorporation tends to be linear up to 3% Al concentration, which could be attributed to the BRUSTEIN-MOSS effect. The excess Al concentration forms an intermediate imperfection level in the energy gap of the pure sample, producing narrowing in it.

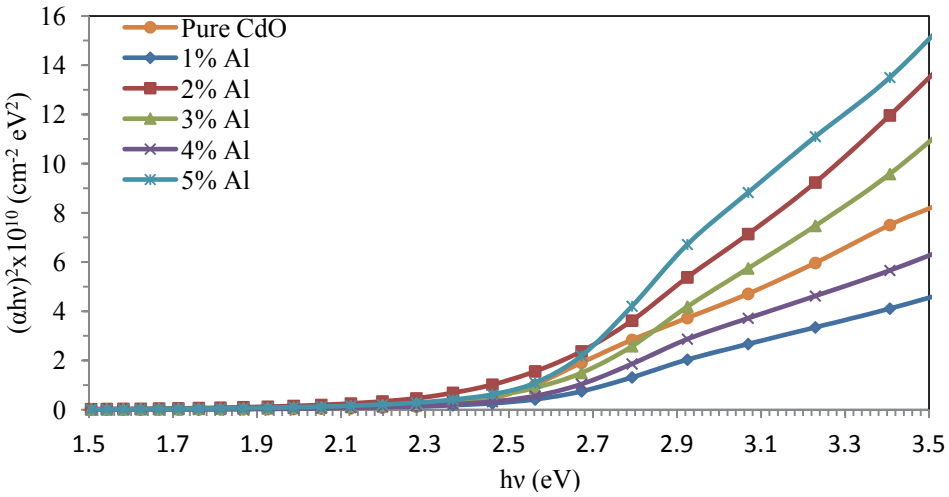

Figure 10. Variation of $(\alpha h\nu)^2$ with photon energy for pure and CdO:Al films.

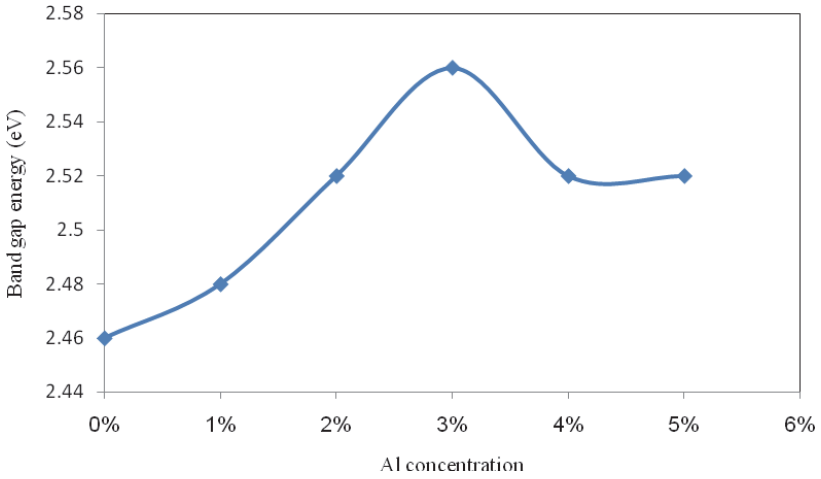

Figure 11. Variation of band gap energy with Al concentrations.

It is observed that the energy of the optical band gaps (E_g) increases with increasing Al incorporation. These results match with that reported in literatures regarding Al-doped CdO obtained using the sol–gel method [10, 25, 38], spray pyrolysis technique [7, 8], and pulsed laser deposition technique [31].

3.2.4 Refractive Index

The refractive indices (*n*) of pure and CdO:Al thin films were determined using the well - known equations [12, 40]:

$$n = \frac{1 + R}{1 - R} + \sqrt{\frac{4R}{(1 - R)^2} - K^2} \tag{5}$$

$$n = \frac{1 + \sqrt{R}}{1 - \sqrt{R}} \tag{6}$$

It is found that the obtained values from both equations are nearly consistent. The change of the refractive index (n) with wavelength of the incident light is given in Figure 12. All samples have the same trend. A slight decrease is observed at wavelength up to 2000 nm beyond an observable increase of (n), depending on the Al concentration. This divergence could be attributed to the increase in free electrons resulting from Al incorporation.

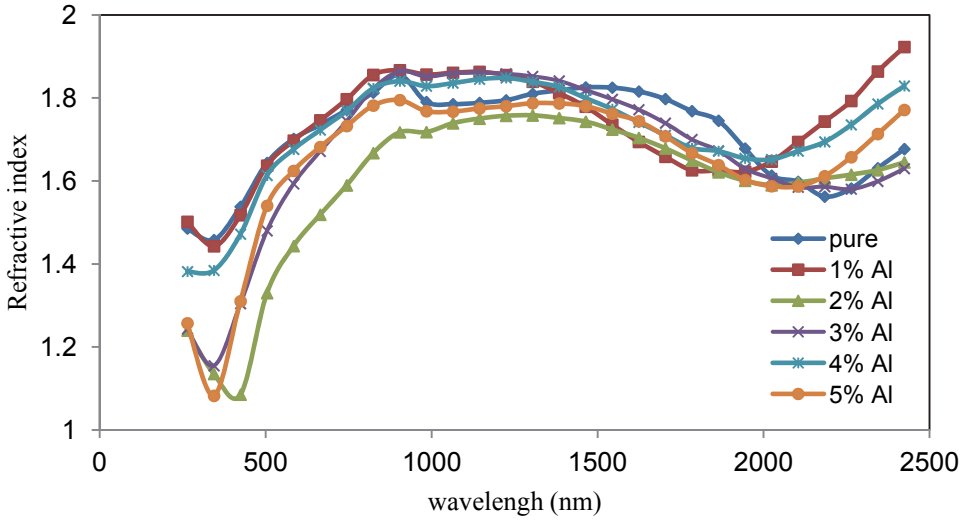

Figure 12. Variation of refractive index with wavelength for films deposited with different Al concentrations.

The calculated values of refractive indices (n) for pure and CdO:Al samples at wavelength 660nm are listed in Table 5. Table 5 also gives the refractive index values of CdOs incorporated with Al, In, and F prepared using different techniques as reported in literature. It is observed that the obtained values are comparable to the values recorded by Abdolahzadeh Ziabari *et al*. [10]. Also, it is observed that the obtained n values are larger than that obtained by Akyuza *et al* [14]. The calculated values are significantly smaller than that reported by Samir A. Maki *et al* [42] and Salih Kose *et al* [12].

Table 5 Variations of the refractive index of the pure & CdO:Al films with different Al concentrations and CdO incorporated Al, In and F prepared previously with different techniques

Doping percentage (%)	Refractive index (n) Present work	Refractive index (n) CdO:Al [10]	Refractive index (n) CdO:Al [42]	Refractive index (n) CdO:In [12]	Refractive index (n) CdO: F [14]
0	1.73	1.81	2.3	4.39	1.42
0.5	-	-	4.1	-	-
1	1.75	1.60	4.7	3.86	-
2	1.52	-	7.2	-	1.39
3	1.73	-	-	2.93	
4	1.73	-	-	-	1.47
5	1.65	1.67	-	2.05	

3. 3 Electrical Properties

The sheet resistance (R_{sh}) of pure CdO and CdO:Al samples was measured using the two probe method. The sheet resistance (R_{sh}) was calculated using the electrical resistance (R) and the dimensions of the sample according to the following equation:

$$R_{sh} = RW / L \tag{7}$$

Where L and W are the length and width of the sample respectively. The variation of sheet resistance (R_{sh}) with Al concentration is shown in Figure 13. The sheet resistance of the samples increases and attains a maximum value of 6 KΩ for the films with 1% Al due to induced electron scattering by incorporated Al atoms. The decrease in sheet resistance by the further increase of Al may be due to the increase in free carriers' concentration. The same trend was observed by C. Aydın and co-workers [26] and by Akyuz *et al.* [8]. Also, a noticeable increase in the resistivity of CdO:F with increasing fluorine doping concentration was recorded by I. Akyuz and co-workers [14]. Salih Kose and co-workers recorded that in doping decreases the conductivity of CdO films [12]

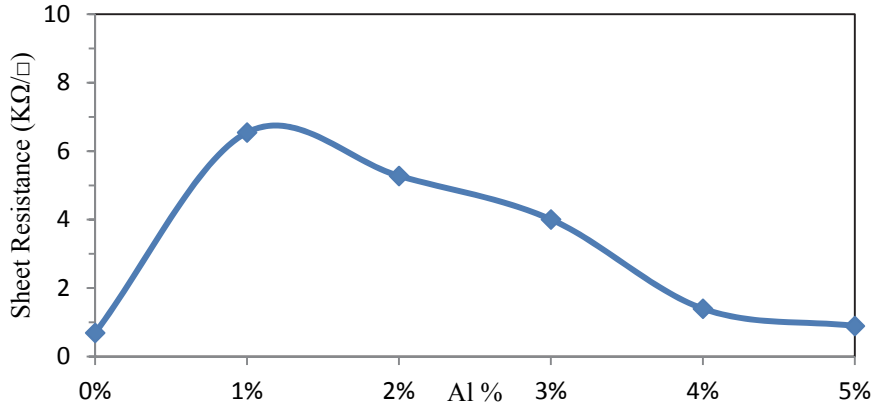

Figure 13. Variation of the sheet resistance with Al concentration for CdO:Al films.

3.4 Figure of Merit

The figure of merit (ϕ) that combines the optical and electrical properties in a single performance quantity is given by the following equation [21]:

$$\phi = T^{10} / R_{sh} \tag{8}$$

Where T is the transmittance and R_{sh} is the sample sheet resistance. The figure of merit is calculated with the transmittance at a wavelength of 660 nm for pure and CdO:Al. The variation of the figure of merit with Al concentration is shown in Table 6. It is seen that, the pure CdO film possesses the highest value of figure of merit. The sheet resistance for Al incorporated CdO films is greater than that of pure CdO, resulting in a low figure of merit.

Table 6 Variation of figure of merit with Al concentration for pure and CdO:Al films

Al concentration (%)	pure	1%	2%	3%	4%	5%
Figure of merit (ϕ)	4.1×10^{-4}	3.96×10^{-6}	2.44×10^{-6}	2.05×10^{-6}	1.47×10^{-5}	5.77×10^{-6}

4. CONCLUSION

Pure CdO and CdO:Al thin films were prepared using the spray pyrolysis method. Aluminum incorporation decreases the pure CdO's crystallinity and changes the growth direction. AFM images show a reasonable increase in surface roughness in samples with low Al concentration, which decreases at higher Al concentration. Energy gap and transmittance values are higher for samples with lower Al concentration than those with a higher one. Crystallite size, microstrain, dislocation density, and refractive index were calculated for the investigated samples. It is inferred that Al incorporation provides amelioration for pure CdO at certain concentrations and deteriorates beyond it.

REFERENCE

[1] Ramiz A. Al-Anssari, Nadir F. Habubi, Jinan Ali Abd, "Fabrication and Characterization of n-Cdo:In/P-Si Thin Film Solar Cell" Journal of Electron Devices **17** (2013) 1457.

[2] M. Zaien, N. M. Ahmed, Z. Hassan "Fabric ation and Characterization of an n-CdO/p-Si Solar Cell by Thermal Evaporation in a Vacuum", Int. J. Electrochem. Sci. **8** (2013) 6988.

[3] Ghaida Salman, Eman Kareem, Asama N. Naje, " Optical and Electrical Properties of CU Doped CdO Thin Films for Detector Applications", International Journal of Innovative Science, Engineering & Technology **1**, 6 (2014) 147.

[4] Y. Yang, Q. Huang, A. W. Metz *et al.*, "Highly Transparent and Conductive CdO Thin Films as Anodes for Organic Light Emitting Diodes: Film Microstructure and Morphology Effects on Performance," Society for Information Display **13**, 5 (2005) 383.

[5] R.K.Gupta, K.Ghosh, R.Patel, P.K.Kahol, "Low Temperature Processed Highly Conducting, Transparent and Wide Band Gap Gd Doped CdO Thin Films for Transparent Electronics", J.Alloys and Compounds **509** (2011) 4146.

[6] R. H. Bari, S. B. Patil, "Nanostructured CdO Thin Films for LPG and CO_2 Gas Sensor Prepared by Spray Pyrolysis Technique", International Letters of Chemistry, Physics and Astronomy **37** (2014) 31.

[7] R. Kumaravel, S. Menaka, S. Regina Mary Snega, K. Ramamurthi, K. Jeganathan, " Electrical, Optical and Structural Properties of Aluminum Doped Cadmium Oxide Thin Films Prepared by Spray Pyrolysis Technique", Materials Chemistry and Physics **122** (2010) 444.

[8] I. Akyuz, S.Kose, F.Atay, V.Bilgin, "Preparation and Characterization of Aluminum-Incorporated Cadmium Oxide Films", Materials Science in Semiconductor Processing **13** (2010) 109.

[9] Arife Gencer Imer, "Investigation of Al Doping Concentration Effect on the Structural and Optical Properties of the Nanostructured CdO Thin Film",Superlattices and Microstructures **92** (2016) 278.

[10] A. Abdolahzadeh Ziabari, F.E. Ghodsi, G. Kiriakidis, " Correlation between Morphology and Electro-optical Properties of Nanostructured CdO Thin Films: Influence of Al Doping", Surface & Coatings Technology **213** (2012) 15.

[11] Ramiz Ahmed Al-Ansari, "Structural, Morphological and Optical Properties of CdO: Al Thin Films Prepared by Chemical Spray Pyrolysis Method", IOSR Journal of Applied Physics **8**, 1 (2016) 06.
[12] Salih Kose, Ferhunde Ataya , Vildan Bilgin, Idris Akyuz, " In Doped CdO Films: Electrical, Optical, Structural and Surface Properties", International journal of hydrogen energy **3,** 4, (2009) S260.
[13] R. Kumaravel, K.Ramamurthi, V.Kris hnakumar, "Effect of Indium Doping in CdO Thin Films Prepared by Spray Pyrolysis Technique", Journal of Physics and Chemistry of Solids, **71** (2010) 1545.
[14] I. Akyuz, S. Kose, E. Ketenci, V. Bilgin, F. Atay, "Optical, Structural and Surface Characterization of Ultrasonically Sprayed CdO:F Films", Journal of Alloys and Compounds **509** (2011) 1947.
[15] Metin Kul, Muhsin Zor, Ahmet Senol Aybek, Sinan Irmak, Evren Turan, " Some Structural Properties of CdO:F Films Produced by Ultrasonic Spray Pyrolysis Method", Thin Solid Film 515 (2007) 8590.
[16] A.A. Dakhel, "Effect of Cerium Doping on the Structural and Optoelectrical Properties of CdO Nanocrystallite Thin Films", Materials Chemistry and Physics **130** (2011) 398.
[17] A. A. Dakhel, "Effect of Tellurium Doping on The Structural, Optical, and Electrical Properties of CdO", Solar Energy 84 (2010) 1433.
[18] M. Thirumoorthia, J. Thomas Joseph Prakash, "A study of Tin Doping Effects on Physical Properties of CdO Thin Films Prepared by Sol–Gel Spin Coating Method", Journal of Asian Ceramic Societies **4** (2016) 39.
[19] A A. Dakhel, "Electrical and Optical Properties of Iron-Doped CdO", Thin Solid Films **518** (2010) 1712.
[20] K. Sankarasubramanian, P.Soundarrajan, T.Logu, S.Kiruthika, K. Sethuraman, R.RameshBabu, K.Ramamurthi, "Influence of Mn Doping on Structural, Optical and Electrical Properties of CdO Thin Films Prepared by Cost Effective Spray Pyrolysis Method", Materials Science in Semiconductor Processing **26** (2014) 346.
[21] R.J. Deokate, S.V. Salunkhe, G.L. Agawane, B.S. Pawar, S.M. Pawar, K.Y. Rajpure, A.V. Moholkar, J.H. Kim, "Structural, Optical and Electrical Properties of Chemically Sprayed Nanosized Gallium Doped CdO Thin Films", Journal of Alloys and Compounds **496** (2010) 357.
[22] K. Usharani,A.R.Balu, V.S.Nagarethinam,M.Suganya, "Characteristic Analysis on the Physical Properties of Nanostructured Mg-Doped CdO Thin Films—Doping Concentration Effect", Progress in Natural Science: Materials International **25** (2015) 251.
[23] A. Bagheri Khatibani, S.M.Rozati, Z.A.Hallaj, "Synthesis and Characterization of Nanostructure CdO:Zn Thin Films Deposited by Spray Pyrolysis Technique: Molarity and Heat Treatment Effects", Materials Science in Semiconductor Processing 16 (2013) 980.
[24] F. Yakuphanoglu, "Synthesis and Electro-optic Properties of Nanosized-Boron Doped Cadmium Oxide Thin Films for Solar Cell Applications", Solar Energy **85** (2011) 2704.
[25] Sinem Aydemir, Salih Kose, M. Selami Kilickaya, Vildan Ozkan, " Influence of Al-doping on Microstructure and Optical Properties of Sol–gel Derived CdO Thin Films", Superlattices and Microstructures **71** (2014) 72.
[26] C. Aydın, H.M. El-Nasser, F. Yakuphanoglu, I.S. Yahia, M. Aksoy, " Nanopowder Synthesis of Aluminum Doped Cadmium Oxide Via Sol–gel Calcination Processing", Journal of Alloys and Compounds **509** (2011) 854.
[27] S. Ilican, M. Caglar, Y. Caglar, F. Yakuphanoglu, "CdO:Al Films Deposited by Sol–gel Process: A Study on Their Structural and Optical Properties", Optoelectronics and Advanced Materials – Rapid Communications **3**, 2 (2009) 135.
[28] A.R. Balu, V.S. Nagarethinam, M. Suganya, N. Arunkumar, G. Selvan, " Effect of the Solution Concentration on the Structural, Optical and Electrical Properties of Silar Deposited CdO Thin Films" Journal of Electron Devices **12** (2012) 739.

[29] Ngamnit Wongcharoen, Thitinai Gaewdang and Tiparatana Wongcharoen, "Electrical Properties of Al-Doped CdO Thin Films Prepared by Thermal Evaporation in Vacuum", Energy Procedia **15** (2011) 361.
[30] Hussein Abdel-Hafez Mohamed, Hazem Mahmoud Ali et al., "Characterization of ITO/CdO/Glass Thin Films Evaporated by Electron Beam Technique. Sci. Technol. Adv. Mater. **9** (2008) 1.
[31] R.K. Gupta, K. Ghosh , R. Patel, S.R. Mishra, P.K. Kahol, "Preparation and Characterization of Highly Conducting and Transparent Al doped CdO Thin Films by Pulsed Laser Deposition", Current Applied Physics **9** (2009) 673.
[32] Qiang Zhou, Zhenguo Ji, BinBin Hu, Chen Chen, Lina Zhao, Chao Wang, "Low Resistivity Transparent Conducting CdO Thin Films Deposited by DC Reactive Magnetron Sputtering at Room Temperature", Materials Letters **61** (2007) 531.
[33] T.P. Gujar, V.R. Shinde,W.Y. Kim, K.D. Jung, C.D. Lokhande, O.S. Joo, "Formation of CdO Films from Chemically Deposited Cd(OH)2 Films as a Precursor", Appl. Surf.Sci **254** (2008) 3813.
[34] Han X, Liu R, Zhude Xu et al. "Annealing Studies on the Structural and Optical Properties of Electrodeposited CdO Thin Films", Electochem. Commun. **7** (2005) 1195.
[35] G. Sivasankar, J. Ramajothi, "Surface Topography, Physical and Optical Properties Studies of Cadmium Oxide (CdO) Thin Film Fabricated by Spray Pyrolysis Technique", International Journal of ChemTech Research **7**, 4 (2014/2015) 1818.
[36] Hassan H. Afify, Ninet M. Ahmed, Magdy Y. Tadros, Fatma M. Ibrahim, "Temperature Dependence Growth of CdO Thin Film Prepared by Spray Pyrolysis", Journal of Electrical Systems and Information Technology **1** (2014) 119.
[37] Ali Jasim Mohammed Al-Jabiry, Muhaj Talib Abdullah, Marwa Abdul Muhsien Hassan, "Piezoelectrical properties for SnO2 thin films prepared by spray pyrolysis method", the International Journal of Nanoelectronics and Materials 7, 2 (2014) 119.
[38] H. H. Afify, S. El- Hefnawi, A. Eliwa, M. Abdel-Naby, N. M. Ahamed, "Preparation of Pure ZnO Films Having an Almost One Plane of Growth", Indian Journal of Physics **79**, 1 (2005) 19.
[39] B G Jeyaprakash, K Kesavan, R Ashok Kumar, S Mohan, A Amalarani, "Temperature Dependent Crystallite-Size and Microstrain of CdO Thin Films Prepared by Spray Pyrolysis Method" , Bull. Mater. Sci. **34**, 4 (2011) 601.
[40] S.J Helen, Sugnanthi Devadason, T. Mahalingam, "Improved Physical Properties of Spray Pyrolysed Al:CdO Nanocrystalline Thin Films" J Mater Sci: Mater Electron **27** (2016) 4426.
[41] Matthew David Femi, Adrian Ohwofosirai, Aboritoli Sunday, Ogah Sunday B. A. Ezekoye F. I. Ezema, R. U. Osuji, "Variation of the Optical Conductivity, Dielectric Function and the Energy Bandgap of CdO using Cadmium Acetate Dehydrat", International Journal of Advances in Electrical and Electronics Engineering **2**, (2), 331..
[42] Samir A. Maki, Alia A.A.Shehab, Ayad A. Salih, "The Optical Properties of Aluminum Doped CdO Thin Films Prepared by Vacuum Thermal Evaporation Technique", Ibn Al-Haitham Jour. for Pure & Appl. Sci. **27**, 3, (2014) 279.